

5
MIP E&F COPY

AD-A201 104

TECHNICAL REPORT BRL-TR-2957

BRL

1938 - Serving the Army for Fifty Years - 1988

APPROACHES TO PENETRATION PROBLEMS

THOMAS W. WRIGHT
KONRAD FRANK

DECEMBER 1988

DTIC
SELECTED
DEC 08 1988
S E D
E

APPROVED FOR PUBLIC RELEASE; DISTRIBUTION UNLIMITED.

U.S. ARMY LABORATORY COMMAND

BALLISTIC RESEARCH LABORATORY

ABERDEEN PROVING GROUND, MARYLAND

88 12 8 035

UNCLASSIFIED
SECURITY CLASSIFICATION OF THIS PAGE

REPORT DOCUMENTATION PAGE				Form Approved OMB No. 0704-0188									
1a. REPORT SECURITY CLASSIFICATION Unclassified		1b. RESTRICTIVE MARKINGS											
2a. SECURITY CLASSIFICATION AUTHORITY		3. DISTRIBUTION/AVAILABILITY OF REPORT APPROVED FOR PUBLIC RELEASE; DISTRIBUTION UNLIMITED											
2b. DECLASSIFICATION/DOWNGRADING SCHEDULE													
4. PERFORMING ORGANIZATION REPORT NUMBER(S) BRL-TR-2957		5. MONITORING ORGANIZATION REPORT NUMBER(S)											
6a. NAME OF PERFORMING ORGANIZATION Ballistic Research Laboratory	6b. OFFICE SYMBOL SLCBR-TB	7a. NAME OF MONITORING ORGANIZATION											
6c. ADDRESS (City, State, and ZIP Code) Aberdeen Proving Ground, MD 21005-5066		7b. ADDRESS (City, State, and ZIP Code)											
8a. NAME OF FUNDING/SPONSORING ORGANIZATION	8b. OFFICE SYMBOL (if applicable)	9. PROCUREMENT INSTRUMENT IDENTIFICATION NUMBER											
8c. ADDRESS (City, State, and ZIP Code)		10. SOURCE OF FUNDING NUMBERS <table border="1"><tr><td>PROGRAM ELEMENT NO.</td><td>PROJECT NO.</td><td>TASK NO.</td><td>WORK UNIT ACCESSION NO.</td></tr></table>			PROGRAM ELEMENT NO.	PROJECT NO.	TASK NO.	WORK UNIT ACCESSION NO.					
PROGRAM ELEMENT NO.	PROJECT NO.	TASK NO.	WORK UNIT ACCESSION NO.										
11. TITLE (Include Security Classification) APPROACHES TO PENETRATION PROBLEMS													
12. PERSONAL AUTHOR(S) Wright, Thomas W. and Frank, Konrad													
13a. TYPE OF REPORT TR	13b. TIME COVERED FROM _____ TO _____	14. DATE OF REPORT (Year, Month, Day)		15. PAGE COUNT									
16. SUPPLEMENTARY NOTATION													
17. COSATI CODES <table border="1"><tr><th>FIELD</th><th>GROUP</th><th>SUB-GROUP</th></tr><tr><td>20</td><td>11</td><td></td></tr><tr><td></td><td></td><td></td></tr></table>		FIELD	GROUP	SUB-GROUP	20	11					18. SUBJECT TERMS (Continue on reverse if necessary and identify by block number) Penetration mechanics, engineering models		
FIELD	GROUP	SUB-GROUP											
20	11												
19. ABSTRACT (Continue on reverse if necessary and identify by block number) Three approaches to penetration mechanics are described; namely, data correlation, numerical simulation, and engineering models. The relative strengths and weaknesses of each are discussed. As an example of the use of engineering models, it is shown how Tate's "modified Bernoulli equation" follows as a consequence of the global balance of mass, momentum, and energy in a steady flow.													
20. DISTRIBUTION/AVAILABILITY OF ABSTRACT <input checked="" type="checkbox"/> UNCLASSIFIED/UNLIMITED <input type="checkbox"/> SAME AS RPT. <input type="checkbox"/> DTIC USERS		21. ABSTRACT SECURITY CLASSIFICATION Unclassified											
22a. NAME OF RESPONSIBLE INDIVIDUAL Thomas W. Wright		22b. TELEPHONE (Include Area Code) 278-6046	22c. OFFICE SYMBOL SLCBR-TB-W										

TABLE OF CONTENTS

	<u>Page</u>
Paragraph 1. INTRODUCTION.	1
2. DATA CORRELATION.	1
3. NUMERICAL SIMULATIONS	3
4. ENGINEERING MODELS.	6
4.1 The Eroding Rod Model: An Example. Conservation Laws.	6
4.2 Conservation Laws Applied to an Eroding Long Rod Penetrator.	8
4.3 Target Response to Cavity Formation	11
4.4 Derivation of the "Modified Bernoulli Equation"	13
4.5 An Approximate Solution	15
5. DISCUSSION AND CONCLUSIONS.	16
LIST OF REFERENCES.	19
DISTRIBUTION LIST	23

Accession For	
NTIS GRA&I	<input checked="" type="checkbox"/>
DTIC TAB	<input type="checkbox"/>
Unannounced	<input type="checkbox"/>
Justification	
By _____	
Distribution/	
Availability Codes	
Dist	Avail and/or Special
A-1	



1. INTRODUCTION

The fundamental problem of penetration mechanics may be stated roughly as follows.

Given a projectile, a target, and details of the initial geometry, kinematics, and materials;

Determine whether or not the target will be perforated upon impact. If perforated, determine what the residual characteristics of projectile and target will be, and if not, determine how deep a hole will be made.

This is an extremely difficult problem, which has defied complete solution for many, many years. It may be approached on at least three different levels: namely, simple data correlation, engineering models of intermediate complexity, or full scale numerical simulation. Data correlations rely on extensive testing, and if good correlations can be found, they may be extremely useful for interpolation to predict other cases that differ only in minor ways from the given data set. However, they cannot be expected to give more than rudimentary insight into the basic physics of the problem since no direct use is made of the balance laws. The construction of engineering models relies on approaches similar to those used successfully in strength of materials and hydraulics. Here simplifying assumptions about kinematics and internal forces are made, and the balance laws for mass, momentum, and energy are satisfied in integral form. At the highest level of complexity, numerical simulation may, in principle, include all the relevant physics, but now other difficulties arise, such as the construction of efficient algorithms for highly distorted materials, and the accurate representation of material behavior.

In this paper, the first and third approach will be briefly commented upon, including some remarks on the strengths and weaknesses of each approach, but the principal emphasis will be placed on the second.

2. DATA CORRELATION

Dimensional analysis, which relies on finding functional relationships among groups of nondimensional parameters, is the principal means for making correlations within large data sets. In the special cases where two dominant groups can be identified (call them x and y), then systematic experimentation can establish a functional relationship between the two in a straight forward way, say $y = f(x)$, where the relationship is valid over as wide a range as one likes. Furthermore, experimentation will usually be made easier by extensive use of subscale models. In ballistic cases, however, it has not been possible to reduce the important nondimensional groups to two or even three. Since the amount of experimentation required to determine a general, unknown, multidimensional function, say $p = f(x,y,z)$, would be prohibitively expensive, a modified approach is usually taken. If it is assumed that the function $f(x,y,z)$ can be fit locally as a power law, that is $f = Ax^a y^b z^c$, where the coefficient A and the exponents a , b , and c are all constants, then after taking logarithms,

the relationship becomes the linear one $\log p = \log A + a \log x + b \log y + c \log z$. In this form, the data can be fit and the constants determined in the standard way with a multilinear regression analysis.

Many examples, which essentially exemplify this approach, may be found in the review article by Backman and Goldsmith.¹ In most cases reported there, the focus is on thin targets and relatively undeformed projectiles, although the same approach is also applicable to thick targets and highly deformed or eroding penetrators. For the most part nondimensional groups have not been used, which tends to limit the applicability of each empirical formula to the specific test data from which it was derived. Neither is it common to use material properties in the correlations.

In a previous review paper² the following formula was given as an example to which the fitting process, outlined above, might be applied.

$$(\rho_p V_L^2 L) / (E_t T \sec \theta) = f(T \sec \theta / D, E_p / E_t, \rho_p / \rho_t, L / D, \dots) \quad (1)$$

In this formula the primary unknown is V_L , the limit velocity at which a penetrator of length L and diameter D will just penetrate a target of thickness T when the angle between the line of flight and target normal is θ . Subscripts p and t stand for penetrator and target, ρ is density and E is a characteristic stress or energy per unit volume. Since $T \sec \theta$ is the path length through the target, the left hand side represents the ratio of available kinetic energy per unit cross sectional area of penetrator to the energy that can be absorbed per unit area of target. Inclusion of the densities and characteristic energies is an attempt to account for material properties in at least a crude way, but there may be other material quantities, such as fracture toughness, that are more significant. The grouping of terms in (1) is plausible, but there may well be other nondimensional arrangements that are more effective. If the right hand side of equation

(1) is replaced by a power law, as suggested previously, Bruchey³ has shown that it is possible to match a limited data set, obtained by various workers at BRL, within about 10%, where the values of the various nondimensional groups vary over ranges of roughly two to five. By choosing other functional forms, as suggested either by a simple engineering theory or by experimental variation of one nondimensional parameter at a time, it is possible to improve the fit to the data considerably. Ongoing efforts in this vein that seem effective for eroding long rod penetrators are being pursued at BRL. This discussion should suffice to indicate at least the nature of uncertainties that are unavoidable in trying to find empirical data correlations.

As a last comment in this section, it has often been noted that if the stress-strain relation for a material is independent of specimen size and rate of deformation, then linear scaling by the same factor for time and all dimensions will leave the equations for balance of momentum invariant. Thus, it should follow that the results of a full scale test can be predicted from those of a subscale experiment, provided that materials are

identical at both scales and that boundary and initial conditions are properly scaled by the same linear factor. In particular, under these conditions the limit velocity in a subscale experiment should be the same as in the full scale test. However, fracture and failure processes are rate dependent in general, as is plastic deformation for many materials. Furthermore, the properties of stock materials tend to vary as thicknesses vary, and the technical details of projectile launch usually preclude exact replicas at full and subscales. Thus, the above idea concerning subscale testing must be used only with great caution. In fact, it has often been observed in our laboratory that limit velocities obtained from small scale tests may be significantly larger than those obtained from full scale tests. There are many vagaries, of course, but this is the trend that would be expected from rate dependent properties, since the natural scaling parameter for rates is given by the striking velocity divided by a characteristic dimension. Thus, smaller scale means higher rate and tougher resistance.

3. NUMERICAL SIMULATIONS

There are several recent review articles that describe the present state of affairs with regard to numerical simulation of impact and penetration^{4,5} so that a comprehensive review will not be attempted here. Instead, it seems worthwhile to make a few comments on general capabilities and limitations and to suggest a few areas where it seems likely that research could pay off in substantially improved capabilities for numerical simulation.

Large scale computations for penetration and impact have been made for well over twenty years. As the size and speed of computers have increased during that time, so has the complexity of codes used for these purposes, but certain characteristic difficulties seem to persist. Lagrangian codes, where the grid points are made to move with the material in which they are embedded, typically fail when cell distortions become too large. The usual regions to give difficulty are in the penetrator ejecta (material that has reversed its direction of motion after impact) and in material near the stagnation point of either penetrator or target where the flow divides and diverges into multiple streams. Consequently, codes of this type have been most useful for examining the response at early times before severe distortions occur. Computational run times can be extended, sometimes dramatically, by various devices. Rezoning (constructing a new computational grid), either by manual intervention or by a continuous and automatic algorithm, have been tried, but the manual method is incredibly time consuming, and automatic means have proven to have limited effectiveness. The ejecta are usually unimportant and are often simply ignored by removing them from the calculation. Material near a stagnation point, however, is usually subject to the highest pressures and rates of distortion in the calculation, and so, it would seem, should hardly be disregarded out of hand. Some sort of local analysis for elastic/plastic materials near a stagnation point might be well worthwhile. Because the grid is fixed in the material, these codes do a particularly good job of keeping track of boundaries between different materials.

Eulerian codes, which use a grid fixed in space, have no difficulty with excessive distortions and so can be made to run for arbitrary lengths

of time, but they do so at the cost of losing distinct material boundaries. This occurs because the fixed grid points do not generally coincide with material boundaries or other free boundaries as the motion progresses, and a kind of averaging process causes a sort of material diffusion across boundaries unless exceptional steps are taken. Since the contact surfaces are often the regions of greatest interest, Eulerian codes are not often used for detailed examination of local events in penetration mechanics. On the other hand, they are used extensively to determine an overall pattern of deformation at longer run times.

Perhaps because of these characteristic problems, until recently, more effort has gone into developing solution algorithms, which sometimes seem to contain rather ad hoc procedures designed more to extend run times than to preserve the integrity of the underlying physics, than has gone into developing appropriate computational models of constitutive behavior.

It is commonly stated by practitioners of computational penetration mechanics that the greatest need is for better material properties. While this is no doubt true as far as it goes, it would be far better to focus attention on the need for better material models since the determination of material properties, as well as their implementation into a particular numerical algorithm, occurs only within the context of some material model. It will be of little use to determine material parameters if the material model used to interpret characterization tests and to implement test results for calculations is inadequate to the task. In fact, as an argument for limiting attention to only the simplest material models, it has sometimes been stated that since the material model will be wrong, it is best to be wrong as cheaply as possible. Some years ago, this attitude resulted in a search for dynamic flow stresses, since most calculations relied only on perfect plasticity. A calculation of the depth of penetration, for example, could then be made to agree with experiment by simply adjusting one material parameter. Although the flow stress calculation today may be more sophisticated, it is common to use an empirical or even arbitrary value for maximum effective shear strain at failure, for example, so again it is possible to fit one experimental measure, deemed to be important, by adjusting a single material parameter. One must then hope that the same value of the parameter will give good results for other calculations and experiments. Economics cannot be ignored, of course, but there is great danger that too narrow a view of material modeling can only be self defeating. As the size and speed of computers increases, it should become feasible to devote substantial computational resources (say, 25 to 30% of computational time) to advanced constitutive models.

The status of material models with relevance for impact calculations was reviewed in a recent report⁶ and the principle conclusions reached then are still valid today. In that report, three elements of material models were discussed; namely, equation-of-state or pressure-volume-temperature response, plastic deformation, and material damage and failure. It was observed that the first area is the most mature and, therefore, requires the least further development, that development of the last is still in its infancy, and that the second is in a state of development intermediate to the other two. It should be noted that material failure models, which treat damage as an internal variable, rely on knowledge of the present

evolution of further damage. In turn, the present state of damage affects the stress calculation. Thus, there is an interaction among all three elements of a material model, and refinement of one element, in particular refinement of the damage model, can be expected to require refinement of the other elements. Because of this, the use of artificial viscosity, which smooths out shock waves in a calculation, should perhaps be reexamined for its effect on the evolution of internal variables.

Within the last five years or so, there has been considerable progress made in several areas of constitutive theory that should have a major influence on impact and penetration calculations. The theory of finite plastic deformation^{7,8,9,10} has recently reached a level of development such that it could be incorporated into penetration codes. For materials that harden isotropically the newer theories are indistinguishable from the classical incremental theory, but a finite deformation theory is essential when plastic anisotropy is involved. For many materials of interest mechanical forming processes, such as rolling, swaging, or extrusion, will produce a texture that is initially anisotropic, and for many others the Bauschinger effect or kinematic hardening will produce it during the deformation.

Detailed models suitable for material damage under dynamic conditions are less advanced than is finite plasticity. Two major classes of damage need to be considered for ductile materials, namely, nucleation and growth of voids under net tension, which leads to spall formation, and formation of adiabatic shear bands under rapid deviatoric motion, which leads to erosion and plugging. In addition, microcracking is another form of damage that is important for brittle materials. Currently there is great activity in developing micromechanical models of all kinds, including these three, and articles on one or the other can be found in almost any current mechanics journal. Emphasis is currently being placed on a detailed treatment at the level of individual features. For use in impact calculations, it will be necessary to abstract a set of internal variables that represent the essential kinetic and kinematic features of the damage and that derive from the micromechanics, and then to apply the results in developing macroscopic constitutive equations, including evolutionary equations for the damage variables.

The most advanced constitutive models for damage during impact have been described by Curran, et al.¹¹ These models all have an extensive empirical basis in that the fundamental kinetic features of the damage variables are assumed, rather than being developed from microscopic considerations. This necessitates that the models be calibrated in rather elaborate dynamic tests where the resulting damage at various stages of evolution is determined by metallurgical examination of the recovered samples. As a consequence it is expensive to calibrate even a single material, and it is difficult to relate the fracture parameters to ordinary physical and mechanical properties. Even so, these models are the best currently available, and they will be used until more refined treatments become available.

Impact codes for treating the high speed collision of solid bodies still have a long way to go before they achieve the level of effectiveness

that is currently available in aerodynamics, for example, where the calculation of high speed flows over bodies of rather complex shape is approaching a level of high art. The same cannot be said for calculations in solid mechanics. In fact, the limit velocity for even the simplest penetrator and target combinations cannot be reliably computed even today, presumably because in the final stages where the penetrator stops just as the target is perforated, all strength, flow, damage, and failure mechanisms come into play in more or less equal measure.

4. ENGINEERING MODELS

The aim of an engineering model is to reduce everything to a simple mathematical form while still retaining the essential physics of the phenomena in question. In penetration mechanics, this results in the representation of a complex and inherently three-dimensional process by a limited number of degrees of freedom so that the result is either a low-dimensional system of ordinary differential equations or at most a few one-dimensional partial differential equations.

There are many potential benefits from such an approach. Basic non-dimensional groups of parameters for scaling may be revealed, which in turn can help tremendously in experimental design, in planning a test series, and in organizing data. With a simple set of equations, solutions can be generated rapidly and perhaps even in closed form for special cases, or else high quality asymptotic solutions may be available. Any of these in turn may suggest an appropriate functional form for improved data correlation and nonlinear regression analysis. Ease of solution also permits systems studies for extensive parametric changes and preliminary full scale design.

On the other hand, reduction to a simple system of equations invariably requires that compromises be made, and that only a limited number of deformation mechanisms be included in the model. For example, at relatively low speeds a blunt projectile may cause structural deformation such as dishing of a thin target element followed by punching of a plug. At higher speeds and with thicker targets there may be extensive deformation or even erosion of the penetrator, and the target may yield without significant structural deformation by first flowing plastically to the side and then by punching only a small plug at the end of the process. The literature is full of examples of this kind. For example, see Goldsmith¹² for an exposition of this point of view, Backman and Goldsmith¹ for a review to that time, and more recently, the work of Ravid and Bodner,¹³ Levy and Goldsmith,¹⁴ Forrestal et al.,¹⁵ Yuan Wenxue, et al.,¹⁶ or Sun Gengshen, et al.¹⁷ There are many other examples in the literature.

4.1 The Eroding Rod Model: An Example. Conservation Laws.

Consider the impact at high speed of a long slender rod on a thick or semi-infinite target. This is the eroding rod model introduced independently by Alekseevski¹⁸ and Tate^{19,20} rediscovered by others since the

1960's, and reviewed by Wright.² The model is here reexamined with special attention being paid to the ever troublesome "modified Bernoulli equation."

By beginning with the full three-dimensional balance laws for mass, momentum, and energy in integral form, an approximate set of one-dimensional penetration equations may be developed. The process is similar in many ways to that used for derivation of the equations of beam theory in solid mechanics or of the equations of hydraulics in fluid mechanics.

A discussion of conservation laws may be found in any standard text on continuum mechanics,^{21,22} and a definitive discussion may be found in the book by Truesdell and Toupin.²³ For present purposes the pertinent facts are recorded below. Any conservation law for a closed, arbitrarily moving region in space simply states that the time rate of accumulation of a conserved quantity, f , within the region in question, is equal to the flux of the quantity transported across the boundary, plus the source of supply, g , at the boundary, plus the source of supply, h , deposited directly in the interior of the region.

$$\frac{d}{dt} \int f dv = \oint f(G - \mathbf{u} \cdot \mathbf{n}) ds + \oint g ds + \int h dv \quad (2)$$

In (2), f , g , and h may have any tensorial character, G is the speed of the surface in the direction of the outward normal, \mathbf{u} is the velocity of the medium, and \mathbf{n} is the outward normal of the surface. The symbol \oint denotes a surface integral. Note that the term $G - \mathbf{u} \cdot \mathbf{n}$ measures the outward speed of the surface relative to the normal speed of the material. Consequently, if no material crosses the surface, the term gives no contribution.

It is essential to include the first term on the right, which gives the contribution due to material convection, in cases such as the eroding penetrator, where the boundary moves relative to the material. Clearly, it is only when the surface is a material boundary that the quantity $G - \mathbf{u} \cdot \mathbf{n} = 0$ identically, and then the convection term vanishes. When the surface is fixed in space, as in a control volume, $G = 0$, and then it gives rise to the Reynold's transport term (see Reference 21). When the fields in question are smooth, since (2) holds for every smooth region in space, it gives rise to the differential balance laws, and when there is a discontinuity, since (2) is assumed to hold in that case as well, it gives rise to the jump laws for shock waves. Equation (2) is written in the spatial form, but of course, it can be transformed into the material form, as well. In the material form the equation looks formally the same, except that in the transport term the quantity $(G - \mathbf{u} \cdot \mathbf{n})ds$ must be replaced by $(\rho_0 / \rho) G_r dS$ where ρ_0 is the original (reference) density, G_r is the outward normal speed of the surface relative to the material in the original configuration, and dS is the surface element in the original configuration. Thus f , g , and h may be referred either to present volumes and areas or to the fixed reference volumes and areas. In applying the integral balance laws below, only the spatial form has been used.

The terms f , g , and h are identified for the three balance laws as follows.

$$\text{Mass: } \frac{d}{dt} \int \rho dv = \oint \rho (G - \underline{u} \cdot \underline{n}) ds, \quad (3)$$

ρ = density, $g = h = 0$.

$$\text{Momentum: } \frac{d}{dt} \int \rho \underline{u} dv = \oint \rho \underline{u} (G - \underline{u} \cdot \underline{n}) ds + \oint \underline{t} \cdot \underline{n} ds + \int \rho \underline{b} dv, \quad (4)$$

$\rho \underline{u}$ = momentum, \underline{t} = Cauchy stress, \underline{b} = body force/unit mass.

$$\text{Energy: } \frac{d}{dt} \int \rho (e + \frac{1}{2} \underline{u} \cdot \underline{u}) dv = \oint \rho (e + \frac{1}{2} \underline{u} \cdot \underline{u}) (G - \underline{u} \cdot \underline{n}) ds + \quad (5)$$

$$+ \oint (\underline{u} \cdot \underline{t} - q) \cdot \underline{n} ds + \int (r + \rho \underline{u} \cdot \underline{b}) dv,$$

e = internal energy/unit mass, q = heat flux, r = energy sources and sinks/unit volume.

4.2 Conservation Laws Applied to an Eroding Long Rod Penetrator

Following Christman and Gehring,²⁴ penetration into a relatively thick target may be idealized as occurring in several stages. Upon first impact a strong shock wave is introduced into both penetrator and target, but due to the presence of nearby free surfaces, the shocks weaken rapidly and soon a quasi-steady flow field is set up near the penetrator/target interface. An attempt to analyse this initial phase approximately has recently been made,²⁵ but the net result in the case of long rods is always that about one to one and a half diameters of rod is eroded. If good estimates of the initial penetration and mass loss in the rod during this first stage of penetration could be made, then the quasi-steady analysis, developed in the sequel, would apply to the remainder of the rod, and to find the total penetration would require that the initial part be added on. Since the approximate analysis is uncertain, a simpler, and not necessarily less accurate, approach is to use the quasi-steady analysis, discussed below, right from the start. In the final stage, either the target material fails and perforation occurs, which requires special treatment, or penetration ceases in a rapid transition from the quasi-steady stage to full rest for all material. Strictly speaking this final stopping stage also should require special treatment.

To consider the second or quasi-steady stage of penetration, refer to Figure 1. In the simplest application of equations (3)-(5) for this stage it is assumed that the material in both penetrator and target behaves as an ideal rigid/perfectly plastic solid. This is the implicit assumption of both Alekseevskii¹⁸ and Tate,^{19,20} but in the present treatment, the role of the energy equation, which has been conspicuous by its absence in past treatments, will be examined, and the modified Bernoulli equation will be cast into a new light. In Figure 1 the rod material is divided into two parts, R and S . In region R the rod is assumed to be rigid and undeformed,

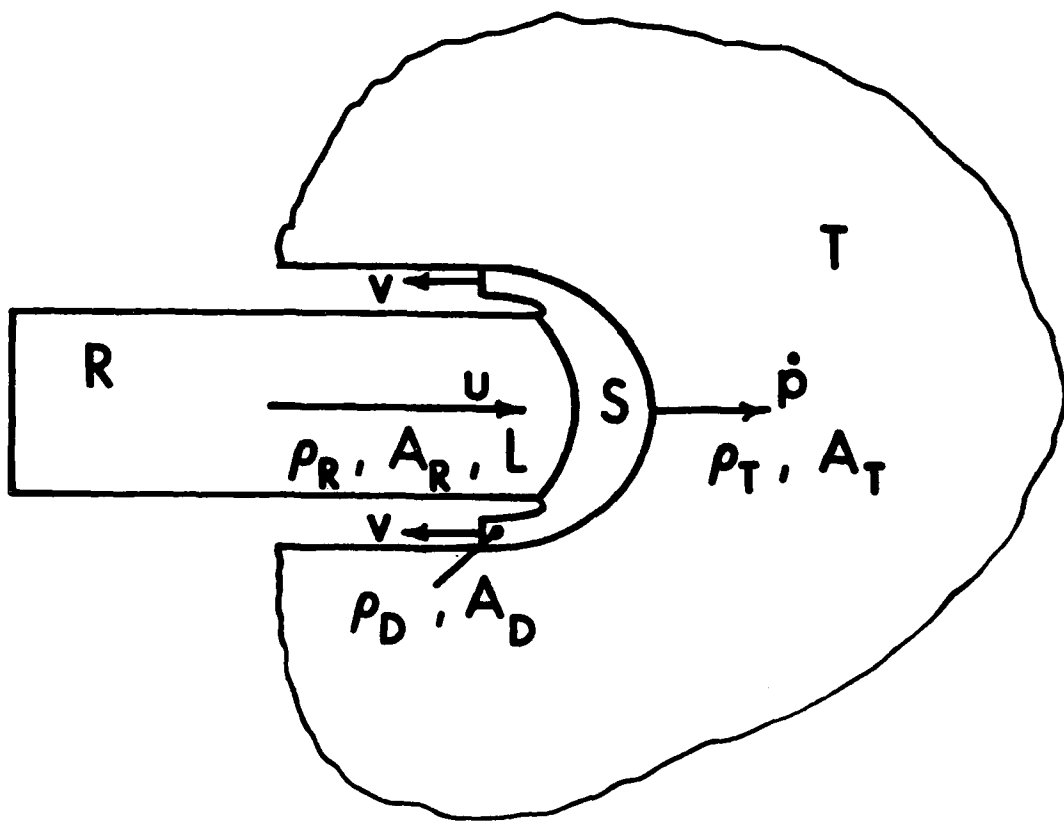


Figure 1. Schematic Diagram of Quasi-Steady Penetration

so that all of the material has speed u in the positive horizontal direction, density ρ_R , cross-sectional area A_R , and instantaneous length L . In region S, which is assumed to be constant in size and shape and to be in a state of steady flow, the material begins to flow plastically at the R-S boundary and then to undergo very large deformations before the debris exits with cross-sectional area A_D , density ρ_D , and velocity v in the rearward or negative horizontal direction. Both the R-S and S-T boundaries simply translate horizontally with speed \dot{p} , where \dot{p} is the depth of penetration. The target material lies in region T and the cross-sectional area of the hole in the target is A_T .

Application of the first two balance laws to region R gives

$$\frac{d}{dt} [\rho_R A_R L] = \rho_R A_R (\dot{p} - u), \quad \text{or} \quad \dot{L} = \dot{p} - u, \quad (6)$$

$$\frac{d}{dt} [\rho_R A_R L u] = \rho_R A_R u (\dot{p} - u) - Y A_R, \quad \text{or} \quad \rho_R L \dot{u} = -Y \quad (7)$$

where γ is the compressive yield stress in the rod, and there is no contribution from the lateral sides of the rod. Because the material has been assumed to be rigid in region R, the only energy is kinetic energy. Thus, the energy law is entirely equivalent to the momentum law and adds nothing new.

The balance laws (3)-(5) applied in succession to the steady region S now give

$$0 = \rho_R A_R (-\dot{p} + u) + \rho_D A_D (-\dot{p} - v) \quad (8)$$

$$0 = \rho_R A_R u (-\dot{p} + u) - \rho_D A_D v (-\dot{p} - v) + F_R + F_D - F_T \quad (9)$$

$$0 = \rho_R A_R (e_R + \frac{1}{2}u^2) (-\dot{p} + u) + \rho_D A_D (e_D + \frac{1}{2}v^2) (-\dot{p} - v) + \int u \cdot t \cdot n \, ds \quad (10)$$

where the left hand sides are all set to zero because of the steady assumption, F_R is the total axial compressive force on the R-S boundary, F_D is the total axial compressive force on the rearward flow of debris, and F_T is the total axial compressive force on the S-T boundary. In (9) e_R and e_D are the densities of internal energy in the rod material at entrance and at exit to region S.

With the notation m for the mass flux, and noting that the velocity may be written $u = \dot{p}e_z + u_r$, where e_z is a unit axial vector and u_r is the velocity relative to the stagnation point, equations (8), (9), and (10) may be rewritten as

$$m = \rho_R A_R (u - \dot{p}) = \rho_D A_D (v + \dot{p}) \quad (11)$$

$$m(u - \dot{p}) + m(v + \dot{p}) = F_T - F_R - F_D = F \quad (12)$$

$$\frac{1}{2}(u - \dot{p})^2 - \frac{1}{2}(v + \dot{p})^2 = -\frac{\gamma}{\rho_R} + \frac{\Sigma_D}{\rho_D} + (e_D - e_R) - \frac{\dot{W}_B}{m} = D \quad (13)$$

In (13) $\dot{W}_B = \int u_r \cdot t \cdot n \, ds$, where integration is taken only over the S-T boundary. Since u_r is tangent to the boundary in a steady flow, \dot{W}_B is a contribution due to shearing tractions on the penetrator-target interface. In arriving at (13), which also could have been obtained directly by using a coordinate system fixed at the front of region S, use has been made of (12) to eliminate the cross-product terms, $u\dot{p}$ and $v\dot{p}$, as well as the $\dot{p}F_T$ term. Then (13) results after division through by m . Also F_R/A_R and F_D/A_D have been written as the average stresses γ and Σ_D . With $(u - \dot{p})$ and $(v + \dot{p})$ renamed U and V and with the right hand sides of (12) and (13) renamed F and D , the equations may be rewritten once again as

$$\rho_R A_R U = \rho_D A_D V \quad (14)$$

$$\rho_R A_R U^2 + \rho_D A_D V^2 = F \quad (15)$$

$$U^2 - V^2 = 2D \quad (16)$$

These have the exact solution

$$U^2 = \frac{1}{2} \frac{(F/\rho_R A_R)^2}{\frac{F}{\rho_R A_R} - D}, \quad V^2 = \frac{1}{2} \frac{\left(\frac{F}{\rho_R A_R} - 2D\right)^2}{\frac{F}{\rho_R A_R} - D}, \quad \frac{U}{V} = \frac{\rho_D A_D}{\rho_R A_R} = \frac{F}{F - 2\rho_R A_R D} \quad (17)$$

4.3 Target Response To Cavity Formation

So far the discussion has focused entirely on the flow of the upsetting rod. To proceed further, attention must now be switched to the flow of the target material around the cavity, and here the discussion becomes much less certain. There seem to be two principal unknowns, namely, the cross-sectional area A_T of the cavity, and the force F_T delivered to the target.

These are related, of course, and must be compatible with the flow field in the target material. In analyzing the rod, advantage could be taken of the interior cylindrical geometry of both the incoming and exiting rod material, where it is reasonable to assume nearly uniform stress and velocity through a cross-section. But in the target, since the flow is exterior to the cavity, nothing is uniform except at large distances from the front of the cavity. This has been a central problem for penetration mechanics, and it has been treated in many different ways, none entirely satisfactory, in an attempt to derive approximate results.

One idea that seems to have been useful is that it takes the same amount of energy to produce a cavity of given volume in a plastic material no matter how the cavity is formed. This led Hill to consider radial cavity expansion (see Hill,²⁶ in which he summarizes his work done during the 1940's). Hopkins²⁷ described dynamic expansion of a spherical cavity, and Goodier²⁸ used these results in a theory of penetration. Later, Hanagud and Ross²⁹ tried to improve on Goodier's result by including compressibility. The idea here is to solve the simpler (but still rather complicated) problem of dynamical expansion of a spherical cavity in an infinite elastic-plastic material, and then to assume that the pressure on the wall of the spherical cavity, weighted by a cosine function, also applies to the case of deep penetration. A further extension of these ideas has been given by Forrestal³⁰ for penetration into dry porous rock. Recently Tate^{31,32} has taken a different tack by considering the flow field produced by a Rankine body. These approaches have all been essentially analytical.

A purely computational approach was begun by Batra and Wright,³³ in which they used the finite element method to investigate the steady flow of an incompressible, rigid/perfectly plastic material past a semi-infinite cavity with hemispherical nose. This is being pursued by Batra,^{34,35} who has since considered the effects of nose shape, work hardening, thermal softening, and rate effects, but not compressibility. For present purposes, the result of all this work is simply to give a variety of estimates, all of unknown reliability, for the coefficients in the formula

$$F_T = A_T(a + bp^2 + cp) . \quad (18)$$

With $c = 0$, this formula seems to have been first applied by Poncelet.³⁶ Sometimes an extra term, proportional to p is added in order to account for rate effects in the target material or perhaps for friction at the interface between rod and target. The p term has been much favored in the Russian literature, e.g. References 37 and 38.

The first coefficient, a , is a hardness number with the dimensions of stress, so it can be expected to be proportional to the compressive stress at first yield. Typical expressions for it are

$$a = (2\Sigma_T/3)[1 + \ln(2E/3\Sigma_T)] + (2\pi^2/27)E_T \quad (\text{Goodier}^{28}) \quad (19.1)$$

$$a = (2\Sigma_T/3)[1 - E_T/E + \ln(2E/3\Sigma_T)] + (2\pi^2/27)E_T \quad (\text{Hanagud and Ross}^{29}) \quad (19.2)$$

$$a = \Sigma_T[2/3 + \ln(2E/3\Sigma_T)] \quad (\text{Tate}^{31}) \quad (19.3)$$

where Σ_T is the simple compressive yield stress, E_T is the plastic tangent modulus (bilinear approximation), and E is the elastic Young's modulus. Typical values for steels from these formulas are about $4\Sigma_T$ to $4.6\Sigma_T$. If these expressions are taken literally for the rigid/plastic approximation, a tends to infinity as E tends to infinity, but Batra and Wright,³³ who only considered the rigid/plastic case, found $a = 3.9\Sigma_T$ numerically. Since the rigid/plastic case is somewhat pathological, requiring volume changes and elastic distortions to vanish, but not pressure or shear stresses, it seems likely that a different limiting process may be required, rather than the straight forward one from (19), in order to achieve a finite limit for a . Batra later found that the numerical value depends strongly on the shape of the cavity, decreasing for a more pointed shape, but experimentally the cavities usually seem close to hemispherical.

The second term is essentially a dynamic pressure term, with b having the dimensions of density, and playing the role of a form or shape drag coefficient. Goodier²⁸ estimated the term to be about ρ_T , but in the calculation of Batra and Wright³³ it came out to be $0.0773\rho_T$. In Batra's

later calculations, where he accounted for strain hardening, strain rate hardening, and thermal softening, as well as nose shape, the coefficient varied by a factor of at least three. Incidentally, in none of those calculations, even those that included a rate effect, was there a strong p term.

The third term, which is identically zero if the flow is truly steady, is analogous to the apparent mass in the flow of perfect fluids around solid bodies. The coefficient, c , has the dimensions of length times density, and was estimated by Goodier²⁸ to be about $(\rho_T d)/3$ where d is the cavity diameter. Thus, the force required to advance the cavity may be written

$$F_T = A_T (a \Sigma_T + b \rho_T p^2 + c \rho_T A_T^{\frac{1}{2}} \ddot{p}) \quad (20)$$

where now the three coefficients a , b , and c are nondimensional numbers that depend on material properties. Considerable research is still needed to pin down these numbers authoritatively. In the unsteady problem it might also be necessary to refine the derivation of equations (8), (9), and (10) since the left hand sides will no longer be identically equal to zero. It seems likely, however, that this may be an unnecessary complication for long rod penetration since the unsteady regimes occur most strongly only at first impact and near termination of penetration.

A major remaining unknown is the cross-sectional area of the cavity. Of course, in the actual flow, the cavity area and shape must adjust themselves so as to balance tractions between penetrator and target everywhere on the interface. Tate³¹ estimated the cavity diameter on the basis of an energy argument, but in the present work, energy balance for region S has already been used, but it did not yield the extra information. It seems clear that careful study of the target flow will be required to clear up this question definitively. It can be argued that during penetrator erosion A_T/A_R must be approximately 2 or greater. (D may be positive or negative, but if it is small, as seems likely in many cases, then equation (17) indicates that A_D/A_R is approximately 1 since ρ_D can be no greater than ρ_R . Then, since A_T is no less than $A_R + A_D$, the result follows.) In any case, the experimental evidence indicates that A_T is nearly constant for a given impact, and that fact is enough to permit further analysis.

4.4 Derivation of the "Modified Bernoulli Equation"

Returning now to equation (17), use of (20) with A_T assumed to be constant, and with F_R , F_D , and D all assumed to be constant as well, (17.1) may be regarded as a first order differential equation for p , or if c in (20) is taken to be zero, as an algebraic equation to be solved for p in terms of u . In either case, when taken together with (6) and (7), the result is a system either of three first order ODE's for L , u , and p , or of

two first order ODE's for L and u . Once the primary integration has been accomplished, p may be found by quadrature, of course. If reliable estimates can be made for the various groupings of constants, integration of such a simple system can easily be done on a microcomputer, although there may be some difficulty when L becomes small since then equation (7) will be stiff.

It is useful to consider special cases, the first being the well known example of perfect fluids. Then there are neither yield stresses nor dissipation terms, and $F_R = F_D = D = 0$. Also $U = V$, and the total force delivered to the target is simply given by $F_T = 2\rho_R A_R U^2$. It happens that in this special case, and in this special case only, there is one more piece of information available, namely, the Bernoulli equation, $p + \frac{1}{2}\rho v^2 =$ constant, which holds pointwise along any streamline in a steady flow. (Here p , ρ , and v are simply generic terms.) By noting that pressure vanishes far from the stagnation point, and by equating pressures at the common stagnation points in the colliding fluid flows, it turns out that $\rho_R U^2 = \rho_T \dot{p}^2$, which may be solved for \dot{p} to give the well known result $\dot{p} = u/(1 + \sqrt{\rho_T/\rho_R})$, and by substitution $F_T = 2A_R \dot{p}^2 = 2A_R \rho_T u^2/(1 + \sqrt{\rho_T/\rho_R})^2$. Here the problem is solved completely except for the cavity diameter, which remains unknown, and if needed, must be found by further investigation of the complete flow problem. In the colliding flow of plastic solids, the simple Bernoulli equation does not hold, because in the integration along a steady streamline, there may be gradients of transverse shear stresses that do not vanish. This point has been discussed by Wright,² by Batra and Wright,³³ and by Pidsley.³⁹

In the case of perfect fluids $D = 0$, and in the case of plastic solids it may still be small. With the rigid plastic assumption e_R must be zero. As the rod material turns and reverses direction, it undergoes intense plastic flow, which converts into heat, and the material usually (but not always) fragments into many small pieces. The term e_D then must account for heating and fracture energy. In steel with density of about 8000 kg/m^3 and specific heat of about $500 \text{ joules/kg/K}^0$ a temperature rise of only 250K^0 corresponds to a flow stress of 1 GPa . In addition, by fragmenting into small pieces, there is virtually unlimited surface energy that could be released. Thus, it seems reasonable to assume that e_D and Y/ρ_R are comparable in size. If the material is highly fragmented, it is also reasonable to set $\Sigma_D = 0$. Finally, due either to local melting or to adiabatic shear on the interface, it seems likely that \dot{W}_B will be small, and in any case, the mass flux m is large. Thus, as an approximation $D = -Y/\rho_R + e_D$, and as a working hypothesis it seems reasonable to assume that D is small compared to $F/\rho_R A_R$. If this is so, then a good approximation to (17.1) is

$$2U^2 = \frac{F}{\rho_R A_R} + D \quad \text{or} \quad (21)$$

$$\frac{1}{2} \rho_R (u - \dot{p})^2 + Y = \frac{1}{4} \rho_T b \frac{A_T}{A_R} \dot{p}^2 + \frac{1}{4} c \rho_T \frac{A_T^{3/2}}{A_R} \ddot{p} + \left[\frac{1}{4} \frac{A_T}{A_R} a \Sigma_T + \frac{1}{2} (Y + \frac{1}{2} \rho_R D) \right] \quad (22)$$

With $c = 0$ in (22) the modified Bernoulli equation of Alekseevskii¹⁸ and Tate^{19,20} has been recovered,

$$\frac{1}{2} \rho_R (u - \dot{p})^2 + Y = \frac{1}{2} \rho_{Te} \dot{p}^2 + R \quad (23)$$

where $\rho_{Te} = \frac{1}{2} \rho_T b \frac{A_T}{A_R}$ is the effective target density. With Goodier's value for b and with $A_T/A_R \approx 2$ the true and effective target densities are nearly equal. The last term on the right hand side of (22), although identified with Tate's target resistance, R , here has an interpretation that differs greatly from Tate's. Note that R is not simply a measure of target hardness, but that it involves characteristics of the rod and of the specific collision under consideration, as well.

Nevertheless, if R is regarded as constant for a particular case, then (23) together with (6) and (7) is the same system of equations as that whose properties were displayed by Tate.^{19,20} In particular, it is known that solutions for total depth of penetration may be expressed in the non-dimensional parametric form

$$\frac{p}{L_0} \sqrt{\frac{\rho_{Te}}{\rho_R}} = S(u_0/c; \rho_{Te}/\rho_R, R/Y) \quad (24)$$

where u_0 is the initial speed of impact, L_0 is the initial length of rod, and $c = \sqrt{Y/\rho_R}$, a characteristic speed determined by material properties. S is a function that is zero for $u_0 < u_c = \sqrt{2(R - Y)/\rho_R}$ (assuming that $R/Y > 1$) and that saturates asymptotically to 1 for large values of u_0 . Equation (24) shows the principle scaling relations in long rod impact, and the dominant nondimensional groupings of physical parameters.

4.5 An Approximate Solution

Although (6), (7), and (23) may be easily integrated on a microcomputer, it is useful to have analytic expressions for either exact or

approximate solutions so that the effect of the various parameters may be more readily exhibited. Recently, Frank and Zook⁴⁰ observed that a good approximation for p , as determined from (23) may be written

$$\dot{p} = \frac{1-\alpha}{1+\mu} u, \text{ where } \mu = \sqrt{\rho_{Te}/\rho_R} \text{ and } \alpha = \frac{c^2}{u^2} = \frac{2(R-Y)}{\rho_R u^2} \quad (25)$$

For values of μ between 0.5 and 2, which is the usual range of interest, equation (25) is correct to within about 5% over the whole range of u , and is exact at the extremes of interest, u_c and ∞ . Frank and Zook⁴⁰ went on to express the solution of (6), (7), and (25) as

$$L/L_0 = n^n \exp[a_o(n-1)], \quad (26)$$

where $n = u^2/u_c^2$, $n = \frac{R/Y - 1}{1 + \mu}$, and $a_o = \frac{\mu u_c^2}{2(1 + \mu)c^2}$

$$p = - \frac{\rho_R}{(1 + \mu)Y} \int_{u_c}^u u L(u) \left(1 - \frac{u_c^2}{u^2}\right) du \quad (27)$$

or $\mu \frac{p}{L_0} = 1 - n^n e^{-a_o(1-n)} - n(1 + \mu) \int_n^1 n^{n-1} e^{-a_o(1-n)} dn$

after changing variables and integrating by parts. In (27) n has the range $n_c = 2(R - Y)/\rho_R u_c^2 \leq n \leq 1$ since penetration stops when $u = u_c$. For given materials μ and n specify the relative material properties and a_o is a measure of the striking velocity. Thus, with $n = n_c$ equation (27) gives the depth of penetration as a function of striking velocity u_c . Since the last integral may be evaluated explicitly for $n = 0, 1, 2, 3, \dots$, expressions may be found that at least outline the expected performance as a function of the dominant material parameters. Furthermore, it provides a functional form, with μ and n as fitting parameters, which should be far more effective in fitting an extended data set than the simple power law form, as discussed in Section 2. This has been amply verified by Frank and Zook.⁴⁰

5. DISCUSSION AND CONCLUSIONS

Three approaches to penetration mechanics have been discussed in this paper. The oldest method, data correlation, is still in wide use today,

and when coupled with the new functional forms, as suggested by simplified engineering models, will continue to be a powerful means for organizing large quantities of data.

In the long run, large scale computing is the only method that can be expected to deal effectively with complex geometric shapes and new configurations outside our usual experience, because it is only in these codes that all relevant physical processes can be included, in principle. The size and speed of modern computers are essential for these calculations, but they are not sufficient. At the present time, our knowledge of large scale flow and fracture processes is still rudimentary and inadequate to the task of a priori prediction in penetration mechanics.

As an example of an effective engineering model, the eroding rod model has been reexamined in some detail. Emphasis has been placed on careful and complete use of the integral form of the balance laws, including energy balance. This ensures that accurate equations of motion will be derived, and it draws attention to the meaning of various terms in the final equations and to the various approximations that have to be made along the way. The assumption of a region of quasi-steady flow of penetrator material has resulted in new understanding of the modified Bernoulli equation. Use of the balance laws focused on the upsetting of the penetrator, and pointed out the need for a better understanding of flow processes in the target material. As with all engineering models, however, the eroding rod model relies on the identification of dominant phenomenology by careful experimentation with the subsequent model being suitably restricted in application.

Only the rigid/perfectly plastic material has been considered, which simplifies the underlying kinematics considerably, but the integral balance laws could equally as well be applied to other material models to obtain penetration equations appropriate for those cases.

LIST OF REFERENCES

1. Backman, M. E. and Goldsmith, W., "The Mechanics of Penetration of Projectiles into Target," *Int. J. Engng. Sci.*, Vol. 16, pp. 1-99, 1978.
2. Wright, T. W., "A Survey of Penetration Mechanics for Long Rods," In J. Chandra and J. E. Flaherty (eds.), *Computational Aspects of Penetration Mechanics*, Springer, New York, pp. 85-106, 1983.
3. Bruchey, W., "Private Communication," 1982.
4. Zukas, J. A., Jonas, G. H., Kimsey, K. D. and Sherrick, T. M., "Three-Dimensional Impact Simulations: Resources and Results," In K. C. Park and R. F. Jones (eds.), *Computer Analysis of Large Scale Structures*, AMD-49, New York: ASME, pp. 35-68, 1981.
5. Anderson, C. E. and Bodner, S. R., "The Status of Ballistic Impact Modeling," 1987, submitted to *Int. J. Impact Engng.*
6. "Materials Response to Ultra-High Loading Rates," Washington: National Materials Advisory Board, NMAB-356, 1980.
7. Anand, L., "Constitutive Equations For Hot Working Of Metals," *Int. J. Plas.*, Vol. 1, pp. 213-232, 1985.
8. Bammann, D. J., "An Internal Variable Model of Viscoplasticity," *Int. J. Engng. Sci.*, Vol. 22, pp. 1041-1053, 1984.
9. Dafalias, Y. F. and Rashad, M. M., "The Plastic Spin Effect on Anisotropic Material Behavior," 1987, *J. Appl. Mech.* (to appear).
10. Onat, E. T., "Representation of Elastic-Plastic Behavior in the Presence of Finite Deformations and Anisotropy," 1987, *Int. J. Plas.* (to appear).
11. Curran, D. R., Seaman, L. and Shockley D. A., "Dynamic Failure of Solids," *Phys. Repts.*, Vol. 147, pp. 253-388, 1987.
12. Goldsmith, W., "Mathematical Modeling of Some Aspects of Plate Perforation," *Trans. 25th Conf. Army Mathematicians*, ARO Report 80-1, pp. 283-372, 1980.
13. Ravid, M. and Bodner, S. R., "Dynamic Perforation of Viscoelastic Plates by Rigid Projectiles," *Int. J. Engng. Sci.* Vol. 21, pp. 577-591, 1983.
14. Levy, N. and Goldsmith, W., "Normal Impact and Perforation of Thin Plates by Hemispherically-Tipped Projectiles - I," *Analytical Considerations*. *Int. J. Impact Engng.*, Vol. 2, pp. 209-229, 1984.
15. Forrestal, M. J., Rosenberg, Z., Luk, V. K. and Bless, S. J., "Perforation of Aluminum Plates With Conical-Nosed Rods," SAND 86- 0292J Albuquerque: Sandia National Laboratory, 1986. (Also, to appear in *J. Appl. Mech.*)

16. Wenzhe, Yuan., Lanting, Zhou., Xiaoqing, Ma., and Stronge W. J., "Plate Perforation by Deformable Projectile - A Plastic Wave Theory," *Int. J. Impact Engng.*, Vol. 1, pp. 393-412, 1983.
17. Gengchen, Sun and Shouheng, Chen, "A Simplified Model of the Normal Impact of a Long Rod Against a Semi-Infinite Target," In J. Morton (ed.), *Structural Impact and Crash Worthiness*, Vol. 11, pp. 61-470. London: Elsevier, 1984.
18. Aleksevskii, V. P., "Penetration of a Rod into a Target at High Velocity," *Comb. Expl. and Shock Waves*, Vol. 2, pp. 99-106 (English Trans.), 1966.
19. Tate, A., "A Theory for the Deceleration of Long Rods After Impact," *J. Mech. Phys. Sol.*, Vol. 15, pp. 387-399, 1967.
20. Tate, A., "Further Results in the Theory of Long Rod Penetration," *J. Mech. Phys. Sci.*, Vol. 17, pp. 141-150, 1969.
21. Lai, W. M., Rubin, D. and Krempl, E., "Introduction to Continuum Mechanics," Oxford: Pergamon, 1978.
22. Gurtin, M. E., "An Introduction to Continuum Mechanics," New York: Academic, 1981.
23. Truesdell, C. A. and Toupin, R. A., "The Classical Field Theories," In H. Flugge (ed.), *Handbuch der Physik*, Band III/1, Berlin-Heidelberg-New York: Springer, 1960.
24. Christman, D. R. and Gehring J. W., "Analysis of High-Velocity Projectile Penetration Mechanics," *J. Appl. Phys.*, Vol. 37, pp. 1579-1587, 1966.
25. Ravid M., Bodner, S. R., and Holzman, I., "Analysis of Very high Speed Impact," *Int. J. Eng. Sci.*, Vol. 25, pp. 473-482, 1987.
26. Hill, R., "Cavitation and the Influence of Headshape In Attack of Thick Targets by Non-deforming Projectiles," *J. Mech. Phys. Sol.*, Vol. 28, pp. 249-263, 1980.
27. Hopkins, H. G., "Dynamic Expansions of Spherical Cavities in Metals," In I. N. Sneddon and R. Hill (eds.), *Progress in Solid Mechanics*, Amsterdam: North-Holland, Vol. I, pp. 85-166, 1960.
28. Goodier, J. M., "On the Mechanics of Indentation and Catering in Solids Targets of Strain-Hardening Metal by Impact of Hard and Soft Spheres," *Proc. 7th Symp. on Hypervel. Impact*, New York: AJAA, Vol. 111 Theory, pp. 215-259, 1965.
29. Hanagud, S. and Ross E., "Large Deformation, Deep Penetration Theory For a Compressible Strain-Hardening Target Material," *AIAA Journal*, Vol. 9, pp. 905-911, 1971.
30. Forrestal, M. J., "Penetration Into Dry Porous Rock," *Int. J. Solids Structures*, Vol. 22, pp. 1485-1500, 1986.

31. Tate, A., "Long Rod Penetration Models - Part 1. A Flow Field Model For High Speed Long Rod Penetration," *Int. J. Mech. Sci.*, Vol. 28, pp. 535-548, 1986.
32. Tate, A., "Long Rod Penetration Models - Part 2. Extensions to the Hydrodynamic Theory of Penetration," *Int. J. Mech. Sci.*, Vol. 28, pp. 599-61, 1986.
33. Batra, R. C. and Wright, T. W., "Steady State Penetration of Rigid Perfectly Plastic Targets," *Int. J. Engng. Sci.*, Vol. 24, pp. 41-54, 1986.
34. Batra, R. C., "Effect of Nose Shape and Strain-Hardening on Steady State Penetration of Viscoplastic Targets," In D. R. J. Owen, E. Hinton and E. Onate (eds.), *Computational Plasticity, Models, Software and Applications*, Swansea:Pineridge, pp. 463-475, 1987a.
35. Batra, R. C., "Steady State Penetration of Viscoplastic Targets," *Int. J. Engng. Sci.*, Vol. 25, 1987b, (to appear).
36. Poncelet, J. V., "Cours de Mecanique Industrielle," Paris, 1829.
37. Agafonov, A. V., "Allowance for Viscosity During Subsonic Penetration of a Solid Body into Isotropic Obstacles," *Sov. Phys. Dokl.*, Vol. 30, pp. 283-284, 1985.
38. Kozlov, V. S., "Penetration Model That Accounts for the Ductile Properties of the Materials of Colliding Bodies," *Problemy Prochnosti*, Vol. 3, pp. 47-52, 1986. (Trans. by Plenum Publ. Corp. pp. 334-341, 1986.)
39. Pidsley, P. H., "A Numerical Study of Long Rod Impact onto a Large Target," *J. Mech. Phys. Sol.*, Vol. 32, pp. 315-334, 1984.
40. Frank, K. and J. Zook, "Energy-Efficient Penetration and Perforation of Targets in the Hyper-Velocity Regime," *Hypervelocity Impact Symposium*, San Antonio, 1986. (Also to appear in *Int. J. Impact Engng.* 5).

DISTRIBUTION LIST

<u>No. of Copies</u>	<u>Organization</u>	<u>No. of Copies</u>	<u>Organization</u>
12	Administrator Defense Technical Info Center ATTN: DDC-DDA Cameron Station Alexandria, VA 22304-6145	3	Commander Armament R & D Center US Army AMCCOM ATTN: SMCAR-SC, J. D. Corrie J. Beetle E. Bloore
4	Director Defense Advanced Research Projects Agency ATTN: Tech Info Dr. E. Van Reuth Dr. G. Farnum Dr. B. Wilcox 1400 Wilson Boulevard Arlington, VA 22209		Dover, NJ 07801-5001
1	Deputy Assistant Secretary of the Army (R & D) Department of the Army Washington, DC 20310	1	Commander Armament R & D Center US Army AMCCOM ATTN: SMCAR-TDC Dover, NJ 07801-5001
1	HQDA DAMA-ART-M Washington, DC 20310	1	Commander Armament R & D Center US Army AMCCOM ATTN: SMCAR-MSI Picatinny Arsenal, NJ 07802-5000
1	HQDA (SARD-TR) Washington, DC 20310	1	Commander Benet Weapons Laboratory ATTN: Dr. E. Schneider Watervliet, NY 12189
1	Commander US Army War College ATTN: Lib Carlisle Barracks, PA 17013	1	Director Benet Weapons Laboratory Armament R & D Center US Army AMCCOM ATTN: SMCAR-LCB-TL Watervliet, NY 12189
1	Commander US Army Command and General Staff College ATTN: Archives Fort Leavenworth, KS 66027	1	Commander US Armament, Munitions and Chemical Command ATTN: SMCAR-ESP-L Rock Island, IL 61229-7300
1	Commander US Army Materiel Command ATTN: AMCDRA-ST 5001 Eisenhower Avenue Alexandria, VA 22333-0001	1	Commander US Army Aviation Research and Development Command ATTN: AMSAV-E 4300 Goodfellow Boulevard St. Louis, MO 63120
1	Commander Armament R & D Center US Army AMCCOM ATTN: SMCAR-LA, T. Davidson Dover, NJ 07801-5001		

DISTRIBUTION LIST

<u>No. of Copies</u>	<u>Organization</u>	<u>No. of Copies</u>	<u>Organization</u>
1	Director US Army Air Mobility Research and Development Command Ames Research Center Moffett Field, CA 94035	2	Commander US Army Mobility Equipment Research & Development Command ATTN: DRDME-WC DRSME-RZT Fort Belvoir, VA 22060
1	Commander US Army Communications Electronics Command ATTN: DELSD-L Fort Monmouth, NJ 07704-5301	1	Commander US Army Natick Research and Development Center ATTN: DRXRE, Dr. D. Sterling Natick, MA 01762
1	Commander US Army Harry Diamond Laboratory ATTN: SLCHD-TA-L 2800 Powder Mill Road Adelphia, MD 20783	1	Commander USAG ATTN: Technical Library Warren, MI 48397-5000
1	Commander US Army Laboratory Command ATTN: AMSLC-TD Adelphia, MD 20783-1145	1	Commander US Army Development and Employment Agency ATTN: MODE-TED-SAB Fort Lewis, WA 98433
1	Commander MICOM Research, Development and Engineering Center ATTN: AMSMI-RD Redstone Arsenal, AL 35898-5500	2	Commander US Army Laboratory Command Materials Technology Laboratory ATTN: SLCMT-MRD, S.C. Chou Watertown, MA 02172-0001
1	Director Missile and Space Intelligence Center ATTN: AIAM-S-YDL Redstone Arsenal, AL 35898-5500	1	Director US Army TRADOC Systems Analysis Activity ATTN: ATAA-SL White Sands Missile Range, 88002
3	Director BMD Advanced Technology Center ATTN: ATC-T, M. Capps ATC-M, S. Brockway ATC-RN, P. Boyd P.O. Box 1500 Huntsville, AL 35807	1	Commandant US Army Infantry School ATTN: ATSH-CD-CSO-OR Fort Benning, GA 31905

DISTRIBUTION LIST

<u>No. of Copies</u>	<u>Organization</u>	<u>No. of Copies</u>	<u>Organization</u>
1	Director US Army Advanced R&D Technology Center ATTN: CRDABH-5, W. Loomis P.O. Box 1500, West Station Huntsville, AL 35807	3	Commander Naval Surface Weapons Center ATTN: Dr. R. Crowe Code R32 Dr. S. Fishman Code X211, Lib Silver Spring, MD 20902-5000
4	Commander US Army Research Office ATTN: Dr. J. Wu Dr. I. Ahmad Dr. G. Anderson P.O. Box 12211 Research Triangle Park, NC 27709	1	Commander and Director US Naval Electronics Laboratory Laboratory San Diego, CA 92152
1	Commander US Army Research and Standardization Group (Europe) Box 65 FPO, NY 09510	5	Air Force Armament Laboratory ATTN: AFATL/DLODL J. Foster John Collins Joe Smith Guy Spitals Eglin AFB, FL 32542-5000
3	Office of Naval Research Department of the Navy ATTN: Dr. Y. Rajapakse Dr. A. Tucker Dr. A. Kushner Washington, DC 20360	1	RADC (EMTLD, Lib) Griffis AFB, NY 13440
3	Commander US Naval Air Systems Command ATTN: AIR-604 Washington, DC 20360	1	AUL (3T-AUL-60-118) Maxwell AFB, AL 36112
1	Commander Naval Sea Systems Command ATTN: Code SEA 62D Department of the Navy Washington, DC 20362-5101	1	Air Force Wright Aeronautical Laboratories Air Force Systems Command Materials Laboratory ATTN: Dr. Theodore Nicholas Wright-Patterson AFB, OH 45433
3	Commander Naval Surface Weapons Center ATTN: Dr. W. H. Holt Dr. W. Mock Tech Lib Dahlgren, VA 22448-5000	1	Director Environmental Science Service Administration US Department of Commerce Boulder, CO 80302
		1	Director Lawrence Livermore Laboratory ATTN: Dr. M. L. Wilkins P. O. Box 808 Livermore, CA 94550

DISTRIBUTION LIST

<u>No. of Copies</u>	<u>Organization</u>	<u>No. of Copies</u>	<u>Organization</u>
7	Sandia National Laboratories ATTN: Dr. L. Davison Dr. P. Chen Dr. W. Herrmann Dr. J. Nunziato Dr. S. Passman Dr. E. Dunn Dr. M. Forrestal P.O. Box 5800 Albuquerque, NM 87185-5800	2	Orlando Technology, Inc. ATTN: Dr. Daniel Matuska Dr. John J. Osborn P.O. Box 855 Shalimar, FL 32579
1	Sandia National Laboratories ATTN: Dr. D. Bamman Livermore, CA 94550	5	SRI International ATTN: Dr. Donald R. Curran Dr. Donald A. Shockey Dr. Lynn Seaman Mr. D. Erlich Dr. A. Florence 333 Ravenswood Avenue Menlo Park, CA 94025
1	Director National Aeronautical and Space Administration Lyndon B. Johnson Space Center ATTN: Lib Houston, TX 77058	2	California Institute of Technology Division of Engineering and Applied Science ATTN: Dr. E. Sternberg Dr. J. Knowles Pasenda, CA 91102
1	Director Jet Propulsion Laboratory ATTN: Lib (TDS) 4800 Oak Grove Drive Pasadena, CA 91103	1	Denver Research Institute University of Denver ATTN: Dr. R. Recht P.O. Box 10127 Denver, CO 80210
1	ETA Corporation ATTN: Dr. D. L. Mykkanen P.O. Box 6625 Orange, CA 92667	1	Massachusetts Institute of Technology Department of Mechanical Engineering ATTN: Prof. L. Anand Cambridge, MA 02139
1	Forestal Research Center Aeronautical Egineering Lab Princeton University ATTN: Dr. A. Eringen Princeton, NJ 08540	3	Rensselaer Polytechnic Institute ATTN: Prof. E. H. Lee Prof. E. Krempl Prof. J. Flaherty Troy, NY 12181
1	Honeywell, Inc. Defense Systems Division ATTN: Dr. Gordon Johnson 600 Second Street, NE Hopkins, MN 55343		

DISTRIBUTION LIST

<u>No. of Copies</u>	<u>Organization</u>	<u>No. of Copies</u>	<u>Organization</u>
2	Southwest Research Institute Department of Mechanical Science ATTN: Dr. U. Lindholm Dr. Charles Anderson 8500 Culebra Road San Antonio, TX 78228	2	Iowa State University Engineering Research Laboratory ATTN: Dr. A. Sedov Dr. G. Nariboli Ames, IA 50010
5	Brown University Division of Engineering ATTN: Prof R. Clifton Prof H. Kolsky Prof L. B. Freund Prof. A. Needleman Prof. R. Asaro Providence, RI 02912	2	Lehigh University Center for the Application of Mathematics ATTN: Dr. E. Varley Dr. R. Rivlin Bethlehem, PA 18015
1	Brown University Division of Applied Mathematics ATTN: Prof. C. Defermos Providence, RI 02912	1	North Carolina State University Department of Civil Engineering ATTN: Prof. Y. Horie Raleigh, NC 27607
2	Carnegie-Mello University Department of Mathematics ATTN: Dr. D. Owen Dr. M. E. Curtin Pittsburgh, PA 15213	1	Rice University ATTN: Dr. C. C. Wang P.O. Box 1892 Houston, TX 77001
5	Cornell University Department of Theoretical and Applied Mechanics ATTN: Dr. Y. H. Pao Dr. A. Ruoff Dr. J. Jenkins Dr. R. Lance Dr. F. Moon Ithaca, NY 14850	4	The John Hopkins University ATTN: Prof. R. Green Prof. W. Sharpe Prof. J. F. Bell Prof. C. A. Truesdell 34th and Charles Streets Baltimore, MD 21218
2	Harvard University Division of Engineering and Applied Physics ATTN: Prof. J. R. Rice Prof. J. Hutchinson Cambridge, MA 02138	1	Tulane University Department of Mechanical Engineering ATTN: Dr. S. Cowin New Orleans, LA 70112

DISTRIBUTION LIST

<u>No. of Copies</u>	<u>Organization</u>	<u>No. of Copies</u>	<u>Organization</u>
3	University of California Department of Mechanical Engineering ATTN: Dr. M. Carroll Dr. W. Goldsmith Dr. P. Naghdi Berkley, CA 94704	3	University of Florida Department of Engineering Science and Mechanics ATTN: Prof. L. Malvern Prof. D. Drucker Prof. E. Walsh Gainesville, FL 32601
1	University of California Department of Aerospace and Mechanical Engineering ATTN: Dr. Y. C. Fung P.O. Box 109 La Jolla, CA 92037	2	University of Houston Department of Mechanical Engineering ATTN: Dr. T. Wheeler Dr. R. Nachlinger Houston, TX 77004
1	University of California at Santa Barbara Department of Mechanical Engineering ATTN: Prof. T. P. Mitchel Santa Barbara, CA 93106	2	University of Illinois Department of Theoretical and Applied Science ATTN: Dr. D. Carlson Prof. D. Scott Stewart Urbana, IL 61801
1	University of California at Santa Barbara Department of Materials Science ATTN: Prof. A. G. Evans Santa Barbara, CA 93106	2	University of Illinois at Chicago Circle College of Engineering Department of Engineering Mechanics and Metallurgy ATTN: Prof. T. C. T. Ting Prof. D. Krojcinovic P.O. Box 4348 Chicago, IL 60690
1	University of California at San Diego Department of Mechanical and Aerospace Engineering ATTN: Prof. S. Nemat Nassar La Jolla, CA 92093	2	University of Kentucky Department of Engineering Mechanics ATTN: Dr. M. Beatty Prof. O. Dillon, Jr. Lexington, KY 40506
1	University of Delaware Department of Mechanical and Aerospace Engineering ATTN: Prof. J. Vinson Newark, DE 19711	2	University of Maryland Department of Mathematics ATTN: Prof. S. Antman Prof. T. P. Liu College Park, MD 20742

DISTRIBUTION LIST

<u>No. of Copies</u>	<u>Organization</u>	<u>No. of Copies</u>	<u>Organization</u>
1	University of Kentucky School of Engineering ATTN: Dean R. M. Bowen Lexington, KY 40506	1	Yale University ATTN: Dr. E. Onat 400 Temple Street New Haven, CT 96520
3	University of Minnesota Department of Engineering Mechanics ATTN: Prof. J. L. Erickson Prof. R. Fosdick Prof. R. James Minneapolis, MN 55455		<u>Aberdeen Proving Ground</u> Dir, USAMSAA ATTN: AMXSY-D AMXSY-MP, H. Cohen
1	University of Missouri-Rolla Department of Engineering Mechanics ATTN: Prof. R. C. Batra Rolla, MO 65401-0249		CDR, USATECOM ATTN: AMSTE-TO-F
1	University of Texas Department of Engineering Mechanics ATTN: Dr. J. T. Oden Austin, TX 78712		CDR, CDEC, AMCCOM ATTN: SMCCR-RSP-A SMCCR-MU SMCCR-SPS-IL
1	University of Washington Department of Aeronautical and Astronautics ATTN: Dr. Ian M. Fyfe 206 Guggenheim Hall Seattle, WA 98195		
1	University of Wyoming Department of Mathematics ATTN: Prof. R. E. Ewing P.O. Box 3036 University Station Laramie, WY 82070		
3	Washington State University Department of Physics ATTN: Prof. R. Fowles Prof. G. Duvall Prof. Y. Gupta Pullman, WA 99163		

USER EVALUATION SHEET/CHANGE OF ADDRESS

This Laboratory undertakes a continuing effort to improve the quality of the reports it publishes. Your comments/answers to the items/questions below will aid us in our efforts.

1. BRL Report Number _____ Date of Report _____

2. Date Report Received _____

3. Does this report satisfy a need? (Comment on purpose, related project, or other area of interest for which the report will be used.)

4. How specifically, is the report being used? (Information source, design data, procedure, source of ideas, etc.)

5. Has the information in this report led to any quantitative savings as far as man-hours or dollars saved, operating costs avoided or efficiencies achieved, etc? If so, please elaborate.

6. General Comments. What do you think should be changed to improve future reports? (Indicate changes to organization, technical content, format, etc.)

CURRENT
ADDRESS

Name _____
Organization _____
Address _____

City, State, Zip _____

7. If indicating a Change of Address or Address Correction, please provide the New or Correct Address in Block 6 above and the Old or Incorrect address below.

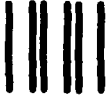
OLD
ADDRESS

Name _____
Organization _____
Address _____
City, State, Zip _____

(Remove this sheet, fold as indicated, staple or tape closed, and mail.)

— — — — — FOLD HERE — — — — —

Director
U.S. Army Ballistic Research Laboratory
ATTN: SLCBR-DD-T
Aberdeen Proving Ground, MD 21005-5066



NO POSTAGE
NECESSARY
IF MAILED
IN THE
UNITED STATES

OFFICIAL BUSINESS
PENALTY FOR PRIVATE USE, \$300

BUSINESS REPLY MAIL
FIRST CLASS PERMIT NO 12062 WASHINGTON, DC
POSTAGE WILL BE PAID BY DEPARTMENT OF THE ARMY

Director
U.S. Army Ballistic Research Laboratory
ATTN: SLCBR-DD-T
Aberdeen Proving Ground, MD 21005-9989



— — — — — FOLD HERE — — — — —